articles

molecular pharmaceutics

Nonviral siRNA Delivery to the Lung: Investigation of PEG−PEI Polyplexes and Their In Vivo Performance

Olivia M. Merkel,[†] Andrea Beyerle,[†,‡] Damiano Librizzi,[§] Andreas Pfestroff,[§] Thomas M. Behr,[§] Brian Sproat,[||] Peter J. Barth,[⊥] and Thomas Kissel*[,†]

Department of Pharmaceutics and Biopharmacy, Philipps Universität Marburg, Ketzerbach 63, 35032 Marburg, Germany, Institute of Lung Biology and Disease, Helmholtz Zentrum München, German Research Center for Environmental Health (GmbH), 85764 Ingolstädter Landstrasse 1, Neuherberg, Germany, Department of Nuclear Medicine, University Hospital Giessen-Marburg, Baldingerstrasse, 35043 Marburg, Germany, Integrated DNA Technologies BVBA, Interleuvenlaan 12A, 3001 Leuven, Belgium, and Institute of Pathology, University Hospital Giessen-Marburg, Baldingerstrasse, 35043 Marburg, Germany

Received April 21, 2009; Revised Manuscript Received May 28, 2009; Accepted July 1, 2009

Abstract: This study describes the physicobiological characterization of PEI− and PEG−PEI polyplexes containing partially 2′-OMe modified 25/27mer dicer substrate siRNAs (DsiRNAs) and their in vivo behavior regarding biodistribution and systemic bioavailability after pulmonary application as well as their ability to knock down gene expression in the lung. Biophysical characterization included circular dichroism of siRNA in polyplexes, condensation efficiency of polymers and in vitro stability. After in vivo application, biodistribution and kinetics of radiolabeled polyplexes were quantified and recorded over time in three-dimensional SPECT images and by end point scintillation counting. The influence on lung tissue and on the humoral and cellular immunosystem was investigated, and finally knockdown of endogenous gene expression in the lung was determined qualitatively. While all of the polymers used in our study were proven to effectively condense siRNA, stability of the complexes depended on the PEG grafting degree. Interestingly, PEI 25 kDa, which showed the least interaction with mucin or surfactant in vitro, performed poorly in vivo. Our nuclear imaging approach enabled us to follow biodistribution of the instilled nanocarriers over time and indicated that PEGylated nanocarriers are more suitable for lung application. While moderate proinflammatory effects were attributed to PEI25k−PEG(2k)$_{10}$ nanocarriers, none of the treatments caused histological abnormalities. Our preliminary in vivo knockdown experiment suggests that PEG−PEI/siRNA complexes are promising nanomedicines for pulmonary siRNA delivery. These results encouraged us to further investigate possible adverse effects and to quantify in vivo gene silencing in the lung after intratracheal instillation of PEG−PEI/siRNA complexes.

Keywords: siRNA; lung; nonviral vectors; SPECT; PEI; lung surfactant; mucin; intratracheal; GFP; knockdown

Introduction

Delivery is still the major hurdle in RNAi therapy. Due to the instability of siRNA and rapid excretion upon systemic injection,[1] most of the clinical trials involving siRNA based drugs utilize local administration to the eyes, targeting macular degeneration and diabetic retinopathy (Acuity Pharmaceuticals, Alnylam Pharmaceuticals, Inc., and Sirna Therapeutics, Inc.), or direct delivery to the brain or the lung (Alnylam Pharmaceuticals, Inc.), and a recent study has demonstrated the advantages of local pulmonary application of both drugs and nucleic acids over systemic iv injection.[2] Lung cancer is already the leading cause of cancer death in the United States[3] and the number 8 cause of death worldwide, while lower respiratory infections are number 3, chronic obstructive pulmonary disease is number 4, and tuberculosis is number 7, according to the World Health

* Corresponding author: Prof. Thomas Kissel, Department of Pharmaceutics and Biopharmacy, Ketzerbach 63, 35032 Marburg, Germany. Tel: +49 6421 28 25881. Fax: +49 6421 28 27016. E-mail: kissel@staff.uni-marburg.de.

[†] Philipps Universität Marburg.

[‡] German Research Center for Environmental Health (GmbH).

[§] Department of Nuclear Medicine, University Hospital Giessen-Marburg.

[||] Integrated DNA Technologies BVBA.

[⊥] Institute of Pathology, University Hospital Giessen-Marburg.

10.1021/mp900107v CCC: $40.75
Published on Web 07/01/2009

Organization (WHO).[4] Therefore, efficient therapies that lead to high and prolonged local drug concentration in the lung are needed to avoid any of these respiratory diseases becoming the number one cause of death. The lung with its vast surface area and strong perfusion is indeed well suited to take up small, hydrophobic drug molecules. It is, on the other hand, only permeable to a limited extent for large, hydrophilic biopharmaceuticals, such as siRNA. Yet, successful local siRNA therapy, e.g. protection from SARS infection,[5] inhibition of RSV[5,6] and influenza A[7] virus replication, has been reported. While most of the in vivo studies of siRNA based therapy used 21mer duplexes that mimic naturally occurring products of Dicer,[8] Kim et al. showed that 27mer blunt double strands can be up to 100-fold more potent than 21mer duplexes.[9] Different approaches to enhance the stability of siRNA have been reported,[10] including modification of the backbone and/or ribose.[11] In particular, methylation of the ribose 2′ hydroxyl group (2′-OMe) offers the additional benefit of diminishing immunostimulatory effects.[12,13] The first study of pulmonary delivery of siRNA reported successful downregulation of heme oxygenase-1 even after application of naked siRNA,[14] and Li et al. only used isotonic dextrose solution (DW5) as carrier.[5] Bitko et al. showed enhanced effects, compared to naked siRNA, with a cationic lipid transfection reagent TransIT-TKO,[6] and in the meantime, a limited number of nanocarriers such as surfactants,[15] mucoadhesive chitosan,[16] and Oligofectamine[17] have been used for improved in vivo pulmonary delivery. In our study, we have investigated how formulation of a 25/27mer 2′-OMe siRNA with polyethylene imine (PEI) and polyethylene glycol (PEG) grafted PEI (PEG−PEI) into nanosized complexes influences biodistribution, absorption, and clearance of vector and load after intratracheal instillation. These parameters were studied by noninvasive nuclear imaging and were compared for PEG−PEIs of different grafting degrees. Additionally, the encapsulation of the modified siRNA, induction of immunostimulatory effects, pulmonary histology after instillation, and finally knockdown of target protein expression were investigated.

Experimental Section

Materials. Poly(ethylene imine), PEI 25 kDa (Polymin, 25 kDa) was a gift from BASF (Ludwigshafen, Germany); the block copolymers poly(ethylene glycol)-poly(ethylene imine) PEI25k−PEG(20k)$_1$ and PEI25k−PEG(2k)$_{10}$[18] were synthesized as described earlier. 2′-O-Methylated 25/27mer DsiRNA targeting EGFP,[19] fluorescent TYE563- and 5′-sense strand C6-amine modified DsiRNA with the same sequence were obtained from Integrated DNA Technologies (Leuven, Belgium); all other reagents were of analytical quality. BALB/c mice were bought from Harlan Laboratories (Horst, The Netherlands), and C57BL/6-Tg(CAG-EGFP)1Osb/J actin-EGFP expressing mice were bought from The Jackson Laboratory (Ben Harbour, ME) and bred in house.

(1) Dykxhoorn, D. M.; Palliser, D.; Lieberman, J. The silent treatment: siRNAs as small molecule drugs. *Gene Ther.* **2006**, *13*, 541–52.

(2) Garbuzenko, O. B.; Saad, M.; Betigeri, S.; Zhang, M.; Vetcher, A. A.; Soldatenkov, V. A.; Reimer, D. C.; Pozharov, V. P.; Minko, T. Intratracheal versus intravenous liposomal delivery of siRNA, antisense oligonucleotides and anticancer drug. *Pharm. Res.* **2009**, *26*, 382–94.

(3) Chandy, D.; Maguire, G.; Aronow, W. S. Lung cancer: the importance of early intervention. *Compr. Ther.* **2009**, *35*, 18–23.

(4) Centre, W. M. *The top 10 causes of death*; World Health Organization: Geneva, 2008.

(5) Zhang, W.; Tripp, R. A. RNA interference inhibits respiratory syncytial virus replication and disease pathogenesis without inhibiting priming of the memory immune response. *J. Virol.* **2008**, *82*, 12221–31.

(6) Bitko, V.; Musiyenko, A.; Shulyayeva, O.; Barik, S. Inhibition of respiratory viruses by nasally administered siRNA. *Nat. Med.* **2005**, *11*, 50–5.

(7) Kwok, T.; Helfer, H.; Alam, M. I.; Heinrich, J.; Pavlovic, J.; Moelling, K. Inhibition of influenza A virus replication by short double-stranded oligodeoxynucleotides. *Arch. Virol.* **2009**, *154*, 109–14.

(8) Hammond, S. M.; Boettcher, S.; Caudy, A. A.; Kobayashi, R.; Hannon, G. J. Argonaute2, a link between genetic and biochemical analyses of RNAi. *Science* **2001**, *293*, 1146–50.

(9) Kim, D. H.; Behlke, M. A.; Rose, S. D.; Chang, M. S.; Choi, S.; Rossi, J. J. Synthetic dsRNA Dicer substrates enhance RNAi potency and efficacy. *Nat. Biotechnol.* **2005**, *23*, 222–6.

(10) Manoharan, M. RNA interference and chemically modified small interfering RNAs. *Curr. Opin. Chem. Biol.* **2004**, *8*, 570–9.

(11) Geary, R. S.; Watanabe, T. A.; Truong, L.; Freier, S.; Lesnik, E. A.; Sioufi, N. B.; Sasmor, H.; Manoharan, M.; Levin, A. A. Pharmacokinetic properties of 2′-O-(2-methoxyethyl)-modified oligonucleotide analogs in rats. *J. Pharmacol. Exp. Ther.* **2001**, *296*, 890–7.

(12) Judge, A. D.; Robbins, M.; Tavakoli, I.; Levi, J.; Hu, L.; Fronda, A.; Ambegia, E.; McClintock, K.; MacLachlan, I. Confirming the RNAi-mediated mechanism of action of siRNA-based cancer therapeutics in mice. *J. Clin. Invest.* **2009**, *119*, 661–73.

(13) Sioud, M.; Furset, G.; Cekaite, L. Suppression of immunostimulatory siRNA-driven innate immune activation by 2′-modified RNAs. *Biochem. Biophys. Res. Commun.* **2007**, *361*, 122–6.

(14) Zhang, X.; Shan, P.; Jiang, D.; Noble, P. W.; Abraham, N. G.; Kappas, A.; Lee, P. J. Small interfering RNA targeting heme oxygenase-1 enhances ischemia-reperfusion-induced lung apoptosis. *J. Biol. Chem.* **2004**, *279*, 10677–84.

(15) Massaro, D.; Massaro, G. D. Critical period for alveologenesis and early determinants of adult pulmonary disease. *Am. J. Physiol.* **2004**, *287*, L715–7.

(16) Kong, X.; Zhang, W.; Lockey, R. F.; Auais, A.; Piedimonte, G.; Mohapatra, S. S. Respiratory syncytial virus infection in Fischer 344 rats is attenuated by short interfering RNA against the RSV-NS1 gene. *Genet. Vaccines Ther.* **2007**, *5*, 4.

(17) Tompkins, S. M.; Lo, C. Y.; Tumpey, T. M.; Epstein, S. L. Protection against lethal influenza virus challenge by RNA interference in vivo. *Proc. Natl. Acad. Sci. U.S.A.* **2004**, *101*, 8682–6.

(18) Petersen, H.; Fechner, P. M.; Fischer, D.; Kissel, T. Synthesis, Characterization, and Biocompatibility of Polyethylenimine-graft-poly(ethylene glycol) Block Copolymers. *Macromolecules* **2002**, *35*, 6867–6874.

(19) Rose, S. D.; Kim, D. H.; Amarzguioui, M.; Heidel, J. D.; Collingwood, M. A.; Davis, M. E.; Rossi, J. J.; Behlke, M. A. Functional polarity is introduced by Dicer processing of short substrate RNAs. *Nucleic Acids Res.* **2005**, *33*, 4140–56.

Polyplex Formation. Polyplexes were formed by mixing equal volumes (25 μL each) of siRNA and polymer diluted in 10 mM HEPES buffer, unless otherwise stated, to obtain the desired nitrogen to RNA phosphate ratio (N/P ratio). Briefly, the appropriate amount of polymer was added to an siRNA solution (2 μM) to yield a final concentration of 1 μM siRNA, vortexed for 10 s and incubated for polyplex formation for 10−20 min.

SYBR Gold Dye Binding Assay. To investigate the condensation of siRNA by the various polymers, 1 μg of EGFP siRNA (IDT, Leuven, Belgium) was complexed with polymers at different N/P ratios and pipetted into opaque FluoroNunc 96 well plates (Nunc, Thermo Fisher Scientific, Langenselbold, Germany). After incubation for 20 min at room temperature, 50 μL of a 1× SYBR Gold solution (Invitrogen, Karlsruhe, Germany) was added to each well and incubated for 10 min in the dark under constant shaking on a sample shaker TH 15 (Edmund Bühler, Hechingen, Germany). Intercalation-caused fluorescence was quantified using a fluorescence plate reader (SAFIRE II, Tecan Group Ltd., Männedorf, Switzerland) at 495 nm excitation and 537 nm emission wavelengths. Experiments were performed in replicates of four, and the results are given as mean relative fluorescence intensity values ± the standard deviation (SD), where intercalation of free siRNA represents 100% fluorescence and non-intercalating SYBR Gold in buffer represents 0% remaining fluorescence.

Fluorescence Quenching Assay. To investigate the condensation efficiency of the polymers used in this study in a direct approach, 1 μg of Tye563-labeled DsiRNA (IDT, Leuven, Belgium) was complexed with polymers at different N/P ratios and pipetted into opaque FluoroNunc 96 well plates (Nunc, Thermo Fisher Scientific, Langenselbold, Germany). Remaining fluorescence was quantified using a fluorescence plate reader (SAFIRE II, Tecan Group Ltd., Männedorf, Switzerland) at 549 nm excitation and 563 nm emission wavelengths. Experiments were performed in replicates of four, and the results are given as mean relative fluorescence intensity values ± SD, where free siRNA represents 100% fluorescence and polymer in buffer represents 0% fluorescence.

Circular Dichroism (CD). To investigate the complexation behavior of the different polymers and their effect on short RNA double strands, we employed circular dichroism spectroscopy, a method widely used in RNA analytics and lately described for characterization of siRNA complexes.[20] Briefly, 2 nmol of siRNA in 100 μL was mixed with 100 μL of polymer solution to form complexes of different N/P ratio. The polyplexes were incubated for 10 min before they were diluted with 200 μL of 10 mM HEPES buffer, pH 7.4 and pipetted into a 0.2 cm quartz cuvette. CD spectra were recorded on a Jasco J 810s spectropolarimeter (Jasco Labor- and Datentechnik GmbH, Gross-Umstadt, Germany) at 20 °C at a scanning speed of 200 nm/min from 200 to 320 nm. As described in ref 20 the response time was 1 s, the bandwidth and data pitch were 1 nm, and each spectrum was accumulated from 5 scans.

Stability of Polyplexes in the Presence of Mucin and Lung Surfactants. Stability of polyplexes was determined by release of siRNA from the complex upon interaction with mucin or Aleveofact, respectively. Therefore, an assay similar to the SYBR Gold dye binding assay was performed with all polyplexes formed at N/P 6. After polyplex formation, 50 μL of a 1× SYBR Gold solution was added and incubated for 10 min in the dark under constant shaking. Afterward, increasing concentrations of mucin (mucin from porcine stomach type II, Sigma-Aldrich Chemie Gmbh, München, Germany) or Alveofact (Boehringer-Ingelheim, Germany) (0−0.33 μg/μL final concentration), respectively, were added and incubated with the polyplexes for another 20 min before fluorescence was quantified using a fluorescence plate reader (SAFIRE II, Tecan Group Ltd., Männedorf, Switzerland) at 495 nm excitation and 537 nm emission wavelengths. Experiments were performed in replicates of four, and the results are given as mean relative fluorescence intensity values ± SD, where free siRNA represents 100% fluorescence and SYBR Gold in buffer represents 0% fluorescence.

In Vivo Biodistribution and Kinetics after Intratracheal Application. All animal experiments were carried out according to the German law of protection of animal life and were approved by an external review committee for laboratory animal care. Polymers and siRNA were radioactively labeled after coupling to p-Bn-SCN-DTPA as previously described.[21,22] Briefly, amine-modified siRNA or polymers, respectively, were mixed with p-Bn-SCN-DTPA at pH 8.5 and reacted for 45 min. Polymers were easily purified using centricon YM-10 spin columns (Millipore, Schwalbach, Germany), and siRNA was precipitated in absolute ethanol and purified using RNeasy Mini columns (Qiagen, Hilden, Germany). DTPA-coupled polymers or siRNA were then incubated for 30 min with $^{111}InCl_3$ (Covidien Deutschland GmbH, Neustadt a.d. Donau, Germany) in 0.1 M sodium acetate buffer, pH 5.4 for radiolabeling before siRNA was purified from free $^{111}InCl_3$ by size exclusion chromatography (SEC) on PD-10 Sephadex G25 (GE Healthcare, Freiburg, Germany) and RNeasy spin column purification, and polymers were purified by SEC only.

(20) Breunig, M.; Hozsa, C.; Lungwitz, U.; Watanabe, K.; Umeda, I.; Kato, H.; Goepferich, A. Mechanistic investigation of poly(ethylene imine)-based siRNA delivery: disulfide bonds boost intracellular release of the cargo. *J. Controlled Release* **2008**, *130*, 57–63.

(21) Merkel, O. M.; Librizzi, D.; Pfestroff, A.; Schurrat, T.; Behe, M.; Kissel, T. In vivo SPECT and real-time gamma camera imaging of biodistribution and pharmacokinetics of siRNA delivery using an optimized radiolabeling and purification procedure. *Bioconjugate Chem.* **2009**, *20*, 174–82.

(22) Merkel, O. M.; Librizzi, D.; Pfestroff, A.; Schurrat, T.; Buyens, K.; Sanders, N. N.; De Smedt, S. C.; Behe, M.; Kissel, T. Stability of siRNA polyplexes from poly(ethylenimine) and poly(ethylenimine)-g-poly(ethylene glycol) under in vivo conditions: Effects on pharmacokinetics and biodistribution measured by Fluorescence Fluctuation Spectroscopy and Single Photon Emission Computed Tomography (SPECT) imaging. *J. Controlled Release* **2009**. DOI: 10.1016/j.jconrel.2009.05.016.

Four to six week old BALB/c mice were anesthetized with xylazine and ketamine and fixed in a supine position on a 60° incline board by holding their upper incisor teeth. The tongue was gently extended using coated tweezers as previously described.[23] Mice were intubated through mouth and trachea using the flexible tube of a 24-gauge catheter (BD Insyte, Becton Dickinson GmbH, Heidelberg, Germany). Polyplexes prepared in PBS containing 35 μg of siRNA and the corresponding amount of polymer for N/P 6 were formed with either radiolabeled siRNA or radiolabeled polymers in order to differentiate between the biodistribution of vector and payload. Polyplexes were incubated for 10 min and instilled into the murine lungs through the BD Insyte tubus. Blood samples were withdrawn retroorbitally 1, 3, 5, 15, 30, 60, and 120 min after instillation. Three-dimensional SPECT and planar gamma camera images were recorded 2, 24, and 48 h after instillation using a Siemens e.cam gamma camera (Siemens AG, Erlangen, Germany) on which a custom built multiplexing multipinhole collimator was mounted. Planar images were analyzed for radioactivity in regions of interest (ROIs) by Syngo software (Syngo, Siemens Medical Solutions, Erlangen, Germany). Dual-isotope SPECT images were recorded 15 min after an additional tail vein injection of 4 MBq ^{99m}Tc-labeled macro-agglomerated albumin (MAA, Mallinckrodt, Hennef/Sieg, Germany). SPECT images were recorded for each isotope separately and later superimposed by the software (Syngo, Siemens Medical Solutions, Erlangen, Germany). After 48 h, animals treated with ^{111}In-labeled polyplexes only were sacrificed and biodistribution of radiolabeled material in dissected organs was measured using a Gamma Counter Packard 5005 (Packard Instruments, Meriden, CT). Radioactive decay of the isotope was factored into the calculations, and results are given as mean percentage of the injected dose (% ID). Control animals either were instilled with PBS only (PBS control) or were anesthetized but not instilled (anesthesia control) in order to assess stress levels caused by bolus instillation or anesthesia, respectively.

Bronchoalveolar Lavage (BAL). Animals were sacrificed 48 h after treatment. BAL was performed as previously described.[24] Briefly, tracheae were cannulated using a BD Insyte catheter, and lungs were rinsed ten times with 1 mL of fresh PBS supplemented with cOmplete Protease Inhibitor Cocktail (Roche Diagnostics, Mannheim, Germany). BAL fluids of each animal were pooled, and the total number of leukocytes captured by lavage was determined using a Casy TT cell counter (Schaerfe Systems, Reutlingen, Germany). Aliquots of 100,000 cells were spun down on glass slides (100*g*, 5 min) to prepare cytospins, and BAL cells were stained for differentiation with Diff-Quick (DADE Diagnostics, Unterschleissheim, Germany). 100 cells were counted and classified concerning morphology and staining. Secretion of 22 pro- and anti-inflammatory cytokines was measured in cell-free BAL fluids by Luminex technology (Luminex System, Bio-Rad Laboratories, Germany) as previously described.[25]

Lung Histology. The influence of exposure of lung tissue to nanomaterials was also examined histologically. Therefore, lungs were inflated via the trachea with and after dissection fixed in a 4% paraformaldehyde solution before they were paraffin-embedded. Paraffin sections (8 μm) were deparaffinized and stained with hematoxylin and eosin (H&E).

In Vivo Knockdown. Four to six week old C57BL/6-Tg(CAG-EGFP)1Osb/J mice were anesthetized with xylazine and ketamine and fixed in a supine position and intubated as described above. Polyplexes containing 50 μg siRNA and the corresponding amount of polymer PEI25k−PEG(2k)$_{10}$ for N/P 6 were formed in 5% glucose solution (total volume per mouse: 50 μL), and instilled into murine lungs using the tubus. Control mice were treated with 5% glucose only. Animals were sacrificed 5 days after instillation, and lungs were inflated with 4% paraformaldehyde, dissected and stored in 4% paraformaldehyde in the dark, before they were embedded in paraffin. The deparaffinized slices (3 μm) were counterstained with 1 μg/mL 4′,6-diamidino-2-phenylindole (DAPI) (Molecular Probes, Invitrogen, Karlsruhe, Germany) solution in PBS for 30 min under light exclusion, and embedded with FluorSave (Calbiochem, Merck Biosciences, Darmstadt, Germany) to protect the fluorophores.

Confocal Laser Scanning Microscopy (CLSM). A Zeiss Axiovert 100 M microscope coupled to a Zeiss LSM 510 scanning device (Zeiss, Oberkochen, Germany) was used for confocal microscopy. For excitation of EGFP fluorescence, an argon laser with an excitation wavelength of 488 nm was used. Fluorescence emission was detected using a 505 nm long-pass filter. Transmission images were obtained in the same scan. In a second scan of the multitrack image, DAPI was detected using a Coherent Enterprise II 653 laser (Coherent, Inc., Santa Clara, CA) with an excitation wavelength of 351 nm and a 385−470 nm bandpass emission filter. All confocal images were acquired with the same settings with respect to laser intensity, filter block, and detector gain.

Flow Cytometric Quantification of Knockdown. C57BL/6-Tg(CAG-EGFP)1Osb/J mice were instilled as described above with 50 μg of siRNA (either siEGFP targeting EGFP or siFLuc targeting firefly luciferase as negative control) complexed with PEI25k−PEG(2k)$_{10}$ at N/P 6. As blanks, C57BL/6 mice not expressing EGFP were treated the same way. Animals were sacrificed 5 days after instillation, exsanguinated and perfused with PBS via the left ventricle. BAL was performed as described above before lungs were

(23) Yu, H.; Buff, S. M.; Baatz, J. E.; Virella-Lowell, I. Oral instillation with surfactant phospholipid: a reliable alternative to intratracheal injection in mouse studies. *Lab. Anim.* **2008**, *42*, 294–304.

(24) Herz, U.; Braun, A.; Ruckert, R.; Renz, H. Various immunological phenotypes are associated with increased airway responsiveness. *Clin. Exp. Allergy* **1998**, *28*, 625–34.

(25) Prabhakar, U.; Eirikis, E.; Reddy, M.; Silvestro, E.; Spitz, S.; Pendley, C., 2nd; Davis, H. M.; Miller, B. E. Validation and comparative analysis of a multiplexed assay for the simultaneous quantitative measurement of Th1/Th2 cytokines in human serum and human peripheral blood mononuclear cell culture supernatants. *J. Immunol. Methods* **2004**, *291*, 27–38.

excised. Lung homogenates were obtained by incubating the excised lungs in 2 mL of a 1 mg/mL Collagenase D solution (Roche, Mannheim, Germany) at 37 °C for 20 min before processing the tissue through a nylon Cell Strainer 100 μm (BD Falcon, Heidelberg, Germany). Cells were then suspended in 10 mL of PBS and centrifuged at 350*g* for 10 min. The supernatant was decanted, and the cells were resuspended, once again centrifuged and resuspended in 500 μL of CellFIX (BD Biosciences, Heidelberg, Germany) for flow cytometry. The residual EGFP expression in the fixed cells was quantified on a FACScan (BD Biosciences, Heidelberg, Germany) flow cytometer with an excitation laser of 488 nm and a bandpass filter of 530/30 nm by counting 10,000 events. Data acquisition and analysis was performed using CellQuest Pro (BD Biosciences, Heidelberg, Germany) and FCS Express V3.00 (DeNovo Software, Thornhill, Canada). Results are given as the average mean fluorescence intensity (MFI) ± SD of the gated viable cells.

Statistics. All analytical assays were conducted in quadruplicate, and all in vivo experiments included 5 animals per group. Results are given as mean values ± standard deviation (SD). Two way ANOVA, statistical evaluation and calculation of the AUC was done using Graph Pad Prism 4.03 (Graph Pad Software, La Jolla, CA).

Results and Discussion

In our earlier study, we had shown that the polymers we used here were all able to condense siRNA into complexes of 150 nm hydrodynamic diameter.[26] Zeta potentials were found to be positive (22 mV for PEI 25k) and slightly decreased for PEG−PEI complexes (15 and 16 mV for PEI(25k)−PEG(2k)$_{10}$ and PEI(25k)−PEG(20k)$_1$, respectively). Stability against RNase degradation and competition with other polyanions has also been described,[26] and serum stability of these complexes has been investigated by fluorescence fluctuation spectroscopy in a later study.[21] In this study, we mainly focused on stability in biological fluids present in the lung such as mucin and surfactants, and we also quantified condensation efficiency of siRNA by the polymers used as follows:

SYBR Gold Dye Binding Assay. Condensation efficiency of the polymers considered that the complexation of nucleic acids which are not accessible to intercalating dyes can be quantified in indirect approaches such as the ethidium bromide quenching assay.[27] Due to the costs of siRNA, SYBR Gold staining, which is 25−100 times more sensitive than ethidium bromide, is much more suitable and gives rise to sufficiently high signals in the micromolar range. In the assays we performed with 1 μg of siRNA (59 pmol), we observed good condensation of siRNA even at low N/P ratios (Figure 1A). Unmodified branched 25 kDa PEI showed full condensation at N/P 1 already, whereas the condensation profiles of the PEGylated PEIs varied depending on their PEGylation pattern. PEI25k−PEG(20k)$_1$ exhibited the worst condensation profile, which corroborates our data obtained in polyacrylamide gel electrophoresis assays (data not shown). This polymer has also been reported to form

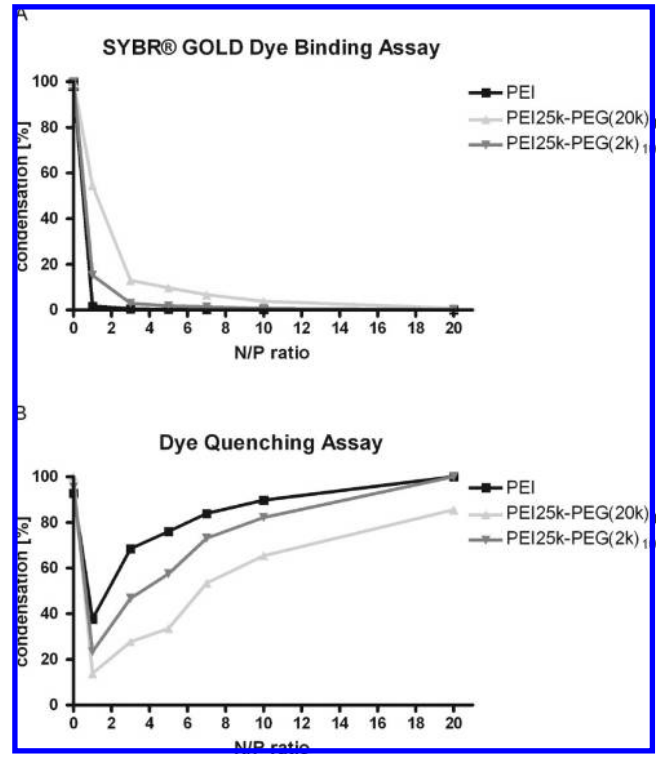

Figure 1. (A) The SYBR Gold dye binding assay revealed very effective encapsulation and protection from intercalation of 2′-OMe DsiRNA. PEI 25 kDa showed the highest efficiency, followed by PEI25k−PEG(2k)$_{10}$ and PEI25k−PEG(20k)$_1$. (B) The dye quenching assay using fluorescently labeled siRNA on the other hand demonstrated a phenomenon earlier described for oligodeoxyribonucleotides.[28] Data obtained by this method therefore has to be interpreted critically.

polyplexes of low stability in the presence of serum.[22] PEI25k−PEG(2k)$_{10}$, on the other hand, showed only slight differences at N/P 1 compared to PEI 25k. The long PEG chain in PEI25k−PEG(20k)$_1$ seems to be disadvantageous for complex formation whereas a higher PEG density of short PEG chains affects complex formation only at low N/P ratios. Unmodified 21mer siRNA was shown to be fully condensed at N/P 3 with all of the polymers used in a recent study.[26] Since gel electrophoresis utilized in the latter report is a more qualitative method, we cannot rule out that slight differences observed in the condensation behavior of unmodified versus 2′-OMe modified siRNA are significant.

Fluorescence Quenching Assay. Another approach for investigating condensation efficiency is the use of assays involving directly labeled nucleic acids that do not require a staining step. Thus, we condensed fluorescently labeled siRNA of the same sequence at the same N/P ratios and the same concentrations as described above. This assay revealed a peculiarity that has previously been described by Van

(26) Mao, S.; Neu, M.; Germershaus, O.; Merkel, O.; Sitterberg, J.; Bakowsky, U.; Kissel, T. Influence of Polyethylene Glycol Chain Length on the Physicochemical and Biological Properties of Poly(ethylene imine)-graft-Poly(ethylene glycol) Block Copolymer/SiRNA Polyplexes. *Bioconjugate Chem.* **2006**, *17*, 1209–18.

Rompaey et al.[28] for oligonucleotide containing poly- and dendriplexes. Interestingly, each curve had a minimum of fluorescence at N/P 1, before fluorescence increased again upon increasing the N/P ratio (Figure 1B). Van Rompaey et al. have described this phenomenon as a reorganization of the polyplexes. They explained that at the minimum of fluorescence a large number of fluorescently labeled molecules are entrapped in one polyplex, quenching each other due to their close spatial proximity. At higher N/P ratios, polyplexes apparently do not "layer up", forming additional layers of polymer on top of the polyplexes, but a redistribution of the number of nucleic acid molecules per polyplex occurs. Therefore, at higher N/P ratios, the number of labeled molecules that are present in one polyplex and trapped in close proximity is decreased, leading to less self-quenching and thus higher intensity fluorescence signals. Van Rompaey et al. had not described this finding for complexation of oligodeoxynucleotides by PEG−PEI, but as previously reported by Glodde et al.,[29] properties of complexes made of the same polymer but different types of nucleic acids may vary considerably. Our findings indicate that, independent of the polymer, at N/P 20 all polyplexes contained so little siRNA that almost no quenching could be observed, although the SYBR Gold dye binding assays proved that siRNA was entrapped and inaccessible for intercalation. Differences between the PEGylated polymers and unmodified PEI 25 kDa were opposite to what has been described above concerning dye binding: PEI 25 kDa had the lowest quenching efficiency, whereas PEI25k−PEG(20k)$_1$ decreased the fluorescence the most. Comparison of both the indirect and the direct approach exhibited properties of a dynamic polyplex−polymer equilibrium that reorganizes according to concentration changes and proved that polyplex formation is not a trivial process. Also the direct approach does not allow for prediction of condensation at a certain N/P ratio. Additionally, we have to keep in mind that, by fluorescent labeling, the siRNA duplex is certainly affected in its chemical properties and might behave differently concerning complexation, even though functionality of the duplex is maintained.

Circular Dichroism (CD). CD is traditionally used to investigate the tertiary structure of nucleic acids. Changes in the spectra can be caused by conformational changes, such as different base stacking which can be observed at the long-wavelength band,[30] and changes at 210 nm which are attributed to backbone conformational transitions.[31] Therefore, this method can also be utilized to investigate variations in the duplex structure caused by electrostatic interaction with polycations. In our study we observed different effects that varied for the three polymers investigated. In general, all spectra recorded had strong resemblance with the A-form of free double stranded RNA characterized by a C3′-endo conformation,[32] which has also been confirmed for 2′-OMe RNA duplexes.[33] One of the effects observed was that PEI 25 kDa, even at low N/P ratios (N/P 1 and 3), caused a slightly decreased Cotton effect (molar ellipticity) at 264 nm compared to that of free siRNA (Figure 2A). Upon increasing the amount of polymer used for complexation (N/P 5−10), the Cotton effect at 264 nm was further decreased, but all spectra for N/P 10, 15, 20, 30, and 40 (N/P 30 and 40 not shown) were very similar, exhibiting a decreased degree of polarization at 264 nm, a very flat curve between 240 and 225 nm and a less negative and slightly red-shifted peak at 210 nm. PEI25k−PEG(20k)$_1$, on the other hand, showed a very strongly decreased Cotton effect at ∼265 nm at N/P 1 which was increased at N/P 3, 5, and 7 (Figure 2B). Complexation at N/P 7 caused only a small decrease of polarization at 264 nm but an extremely flat curve between 240 and 225 nm and the strongest effects at 210 nm, where the slight minimum was red-shifted. Upon increasing the N/P ratio, this effect was reversed. Curves at N/P 10, 15, and 20 were very similar, as observed with PEI 25k. This again could be a sign of a reorganization process depending on polymer concentration, as observed in the dye quenching assay, with the strongest effects on backbone conformation (210 nm) observed at N/P 7. As shown in Figure 2C, PEI25k−PEG(2k)$_{10}$ caused a decreased Cotton effect at 264 nm at all N/P ratios, and curves were similar from N/P 1 up to N/P 20 being comparable to the curves observed with PEI 25k. These findings indicated that all of our polymers did interact with siRNA leading to changes in backbone conformation and base stacking. The disappearance of the negative peak at 210 nm has, on the other hand, previously been attributed to high concentrations of PEG, due to an overlapping, positive CD band at shorter wavelengths.[34] But if PEG was the reason, the phenomenon would be accompanied by an up to 12.5-fold increase of the maximum at 264 nm shifted to 270 nm. Since this was not observed, but the negative peak also disappeared upon complexation with PEG-free PEI 25 kDa, we hypothesize that it was caused

(27) Germershaus, O.; Mao, S.; Sitterberg, J.; Bakowsky, U.; Kissel, T. Gene delivery using chitosan, trimethyl chitosan or polyethylenglycol-graft-trimethyl chitosan block copolymers: establishment of structure-activity relationships in vitro. *J. Controlled Release* **2008**, *125*, 145–54.

(28) Van Rompaey, E.; Engelborghs, Y.; Sanders, N.; De Smedt, S. C.; Demeester, J. Interactions between oligonucleotides and cationic polymers investigated by fluorescence correlation spectroscopy. *Pharm. Res.* **2001**, *18*, 928–36.

(29) Glodde, M.; Sirsi, S. R.; Lutz, G. J. Physiochemical properties of low and high molecular weight poly(ethylene glycol)-grafted poly(ethylene imine) copolymers and their complexes with oligonucleotides. *Biomacromolecules* **2006**, *7*, 347–56.

(30) Gray, D. Circular Dichroism of Protein−Nucleic Acid Interactions. In *Circular Dichroism and the Conformational Analysis of Biomolecules (The Language of Science)*; Fasman, G., Ed.; Plenum Press: New York, 1996; pp 469−500.

(31) Woody, R. W. Circular dichroism. *Methods Enzymol.* **1995**, *246*, 34–71.

(32) Saenger, W. *Principles of Nucleic Acid Structure*; Springer-Verlag: Berlin, 1984.

(33) Inoue, H.; Hayase, Y.; Imura, A.; Iwai, S.; Miura, K.; Ohtsuka, E. Synthesis and hybridization studies on two complementary nona(2′-O-methyl)ribonucleotides. *Nucleic Acids Res.* **1987**, *15*, 6131–48.

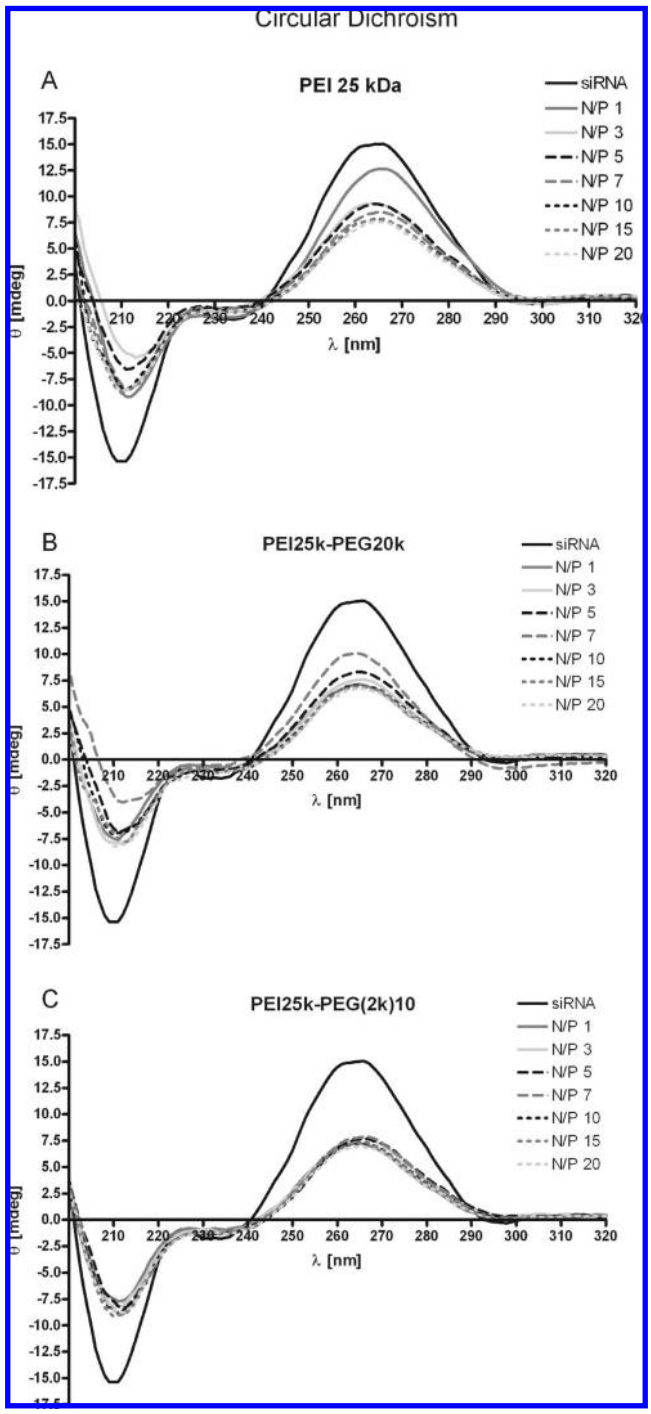

Figure 2. Circular dichroism (CD) spectroscopy emphasized differences in the condensation behavior of the various polymers. While PEI 25 kDa (A) showed increasing condensation with increasing polymer concentration, PEI25k−PEG(20k)$_1$ (B) caused a minimum of condensation at N/P 7, and PEI25k−PEG(2k)$_{10}$ (C) had almost the same effect on siRNA at every N/P tested.

by complexation dependent changes in the backbone conformation. In contrast to spermine, a tetravalent polycation which was reported to stabilize the A-form of dsRNA by increasing the intensity of the positive band at 264 nm in a concentration range between N/P 1 and 10,[35] all of our polycations destabilized the base stacking of the siRNA. While the same report also described an increase of intensity of the negative band at 210 nm, Steely et al. explained that a decrease of intensity at 210 nm is related to condensation of dsRNA.[36] In our study, we showed that while concentration dependent effects were different for each polymer, siRNA nucleobase stacking and backbone conformation were influenced upon complexation with each polymer at every single N/P ratio corroborating the results from the SYBR Gold assay.

Stability Assay in the Presence of Mucin and Lung Surfactants. Stability of nanocarriers in biological fluids is a major limitation for systemic application and was found to be insufficient for PEI or PEG−PEI polyplexes.[22] Due to decreased nuclease activity in the lung, even naked siRNA yielded successful knockdown of gene expression,[14,37] but formulations of siRNA were expected to overcome several barriers present in the lung allowing reduction of the applied dose by increasing the active concentration in the cytosol, thus limiting adverse side effects. Before contact with the airway cell membranes occurs, however, nanocarriers need to penetrate the mucus layer, the surfactant layer, and the periciliary fluid layer covering the airway cells,[38] all of which pose considerable biomechanical hurdles in pulmonary siRNA delivery. To investigate whether polyplexes could penetrate the airway lineaging fluids as intact nanocarriers, we performed SYBR Gold staining assays in the presence of Alveofact or mucin, respectively, to quantify the release of siRNA from polyplexes. Reduced stability of pDNA/PEI complexes compared to pDNA/TAT−PEG−PEI complexes was observed in the presence of surfactant or BAL fluid,[38] yet siRNA complexes showed different stability profiles. After an incubation period of 20 min, PEI complexes were more stable in the presence of surfactant or mucin than PEG−PEI complexes, as shown in Figure 3. While PEI complexes released only 2.5% of their payload in 0.33 mg/mL mucin and 1.0% in 0.33 mg/mL surfactant, PEI25k−PEG(20k)$_1$ complexes were less stable and released 34.1% and 15.8% in 0.33 mg/mL mucin and surfactant respectively. The PEI25k−PEG(2k)$_{10}$ complexes exhibited

(34) Evdokimov, Y. M.; Pyatigorskaya, T. L.; Polyvtsev, O. F.; Akimenko, N. M.; Kadykov, V. A.; Tsvankin, D. Y.; Varshavsky, Y. M. A comparative X-ray diffraction and circular dichroism study of DNA compact particles formed in water-salt solutions, containing poly(ethylene glycol). *Nucleic Acids Res.* **1976**, *3*, 2353–66.

(35) Minyat, E. E.; Ivanov, V. I.; Kritzyn, A. M.; Minchenkova, L. E.; Schyolkina, A. K. Spermine and spermidine-induced B to A transition of DNA in solution. *J. Mol. Biol.* **1979**, *128*, 397–409.

(36) Steely, H. T., Jr.; Gray, D. M.; Lang, D. Study of the circular dichroism of bacteriophage phi 6 and phi 6 nucleocapsid. *Biopolymers* **1986**, *25*, 171–88.

(37) Li, B. J.; Tang, Q.; Cheng, D.; Qin, C.; Xie, F. Y.; Wei, Q.; Xu, J.; Liu, Y.; Zheng, B. J.; Woodle, M. C.; Zhong, N.; Lu, P. Y. Using siRNA in prophylactic and therapeutic regimens against SARS coronavirus in Rhesus macaque. *Nat. Med.* **2005**, *11*, 944–51.

(38) Rubin, B. K. Physiology of airway mucus clearance. *Respir. Care* **2002**, *47*, 761–8.

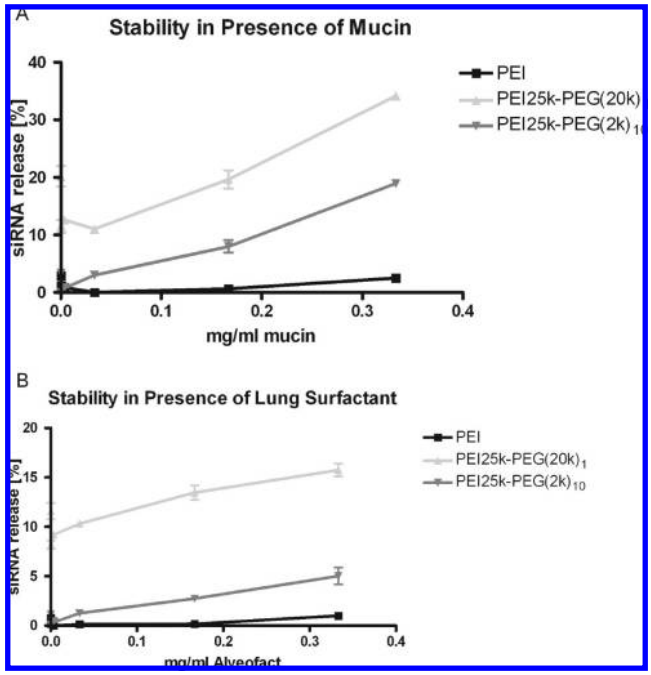

Figure 3. Stability of polyplexes in the presence of (A) mucin and (B) lung surfactant was the highest for unmodified PEI, followed by PEI25k−PEG(2k)$_1$ and PEI25k−PEG(20k)$_1$. This trend corroborates observations made in the presence of serum[22] but does not solely determine suitability for pulmonary application.

intermediate stability with release of 18.9% and 5.0% of their payload in 0.33 mg/mL mucin and surfactant respectively. The same trend had been shown earlier concerning stability in the presence of serum.[22] Unmodified PEI formed the strongest complexes in terms of electrostatic interactions, while this interaction is decreased in PEGylated PEIs, where noncharged PEG chains are present which are hypothesized to hinder complex formation. In vivo, on the other hand, these electrostatically formed complexes can dissociate when high concentrations of competing polyanions are present. Further, it has to be noted that electrolyte complexes which are stable in vitro are not necessarily resistant to interaction with other charged components,[39] while this is a property of sterically shielding complexes.[29]

In Vivo Biodistribution and Kinetics after Intratracheal Application. As previously described,[21,22] radiolabeling nanocarriers with γ-emitters such as ^{111}In enables noninvasive three-dimensional imaging. Dual-isotope SPECT imaging was applied to noninvasively prove instillation into the lungs in living animals by colocalization of ^{111}In-labeled nanocarriers and ^{99m}Tc-labeled macroagglomerated albumin (MAA), which is routinely used in the clinics for lung perfusion

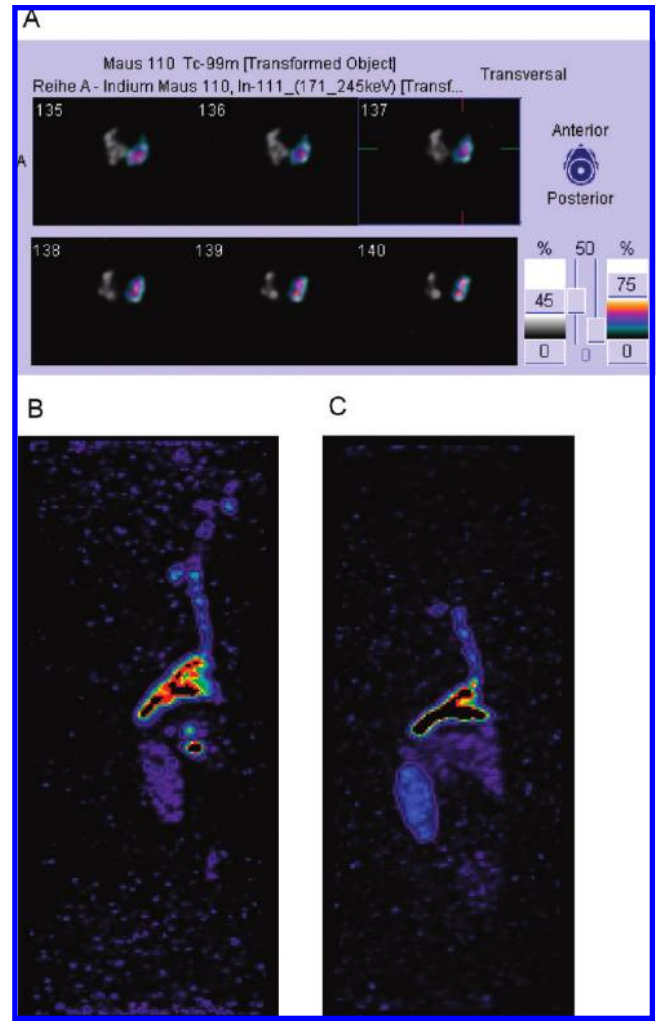

Figure 4. (A) Dual-isotope SPECT imaging of mice treated with ^{111}In-labeled PEI25k−PEG(2k)$_{10}$/siRNA polyplexes and ^{99m}Tc-labeled MAA allowed for control of intratracheal application in the living animal. (B) 3D-SPECT after 24 and (C) 48 hours post instillation showed slow elimination of radiolabeled polymer via the kidneys and circumvention of the first pass effect.

imaging due to accumulation in airway capillaries.[40] Since the SYBR Gold assays had revealed good condensation and the dye quenching assay had proven sufficient loading in terms of molecules of siRNA per polyplex, an N/P 6 was chosen for in vivo application which had been well tolerated in studies where polyplexes were applied intravenously.[21,22] Dual-isotope SPECT, shown in Figure 4A, proved noninvasively by colocalization of the ^{99m}Tc signal (grayscale) and the ^{111}In signal (color) that the radiolabeled polyplexes were applied to the lungs. Interestingly, in some animals, a larger part of the dose was directed to the left lobe, which is also

(39) Burke, R. S.; Pun, S. H. Extracellular barriers to in Vivo PEI and PEGylated PEI ated gene delivery to the liver. *Bioconjugate Chem.* **2008**, *19*, 693–704.

(40) Shih, W. J.; Robinson, M. C.; Huber, C.; Pulmano, C. Tc-99m MAA lung perfusion scintigraphy performed before and after pulmonary embolectomy for saddle-type pulmonary embolism. *Clin. Nucl. Med.* **1995**, *20*, 128–31.

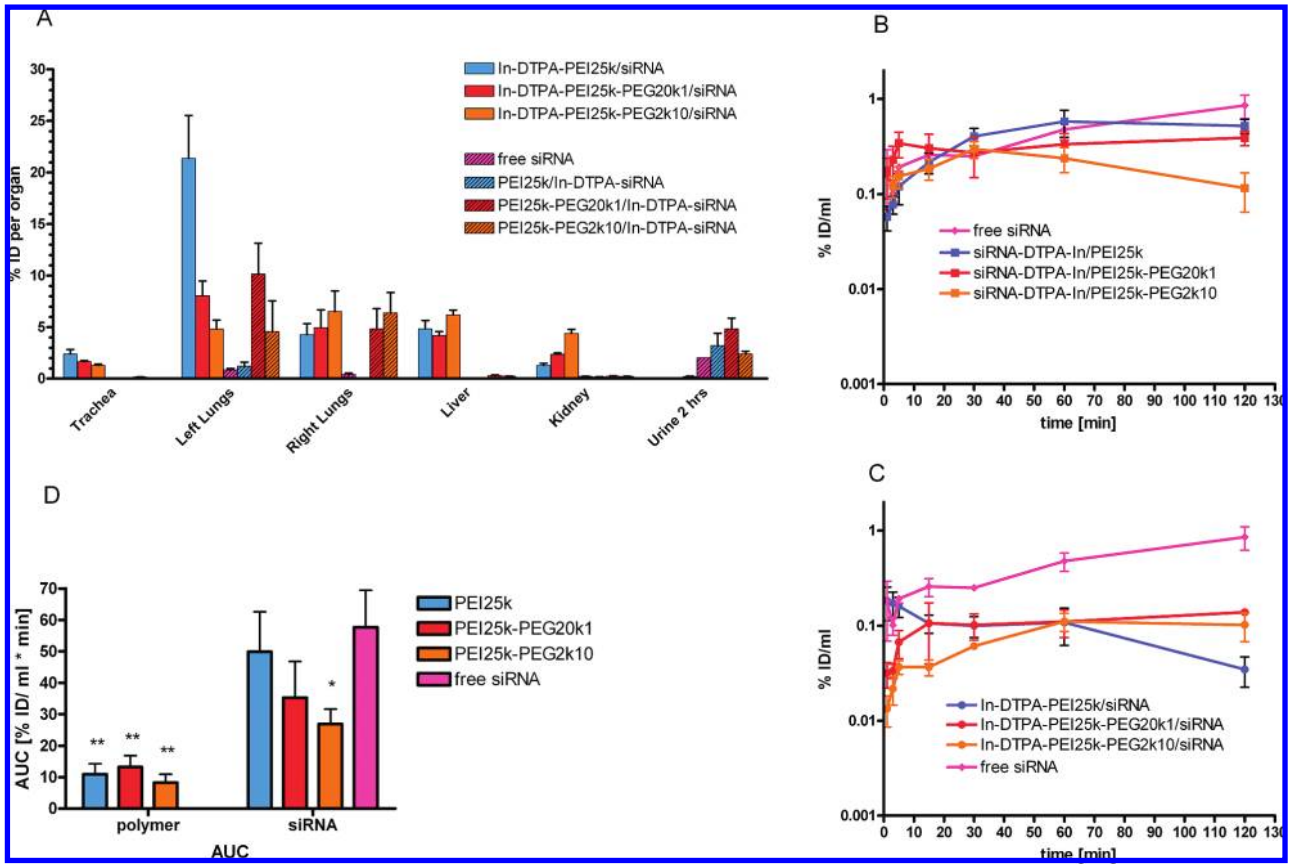

Figure 5. (A) Biodistribution of radiolabeled polymeric vectors and their payload measured in dissected organs 48 h post instillation revealed that the highest signals were still found in the lungs, whereas liver deposition of polymers was about 5% ID and siRNA was rather excreted than accumulated. (B) Systemic bioavailability of labeled siRNA complexed with PEI 25 kDa increased strongly 30 min post instillation, while PEG−PEI complexed siRNA showed higher blood levels immediately after application and did not further increase or even decreased over time. (C) Radiolabeled polymers were retained more strongly in the lung (PEI 25 kDa) or accumulated slightly in the kidneys (PEG−PEIs) and showed lower blood levels than siRNA. (D) AUC values of labeled polymers were accordingly significantly (**$p < 0.01$) lower than those of labeled siRNA. PEI25k−PEG(2k)$_{10}$ complexed siRNA also exhibited a lower AUC value, caused by excretion to the urine.

shown in Figure 4A, and depends on the position of the tubus during instillation and on the anatomy of the murine lung.[41] Variations in airway branching patterns in mammals are known to contribute to differences in regional deposition in the lungs.[42,43] Three-dimensional (3D) SPECT images of mice that were only treated with ^{111}In-labeled polyplexes (but not with MAA) were taken 2, 24, and 48 h after instillation to monitor biodistribution and clearance of the applied polyplexes. As demonstrated in Figure 4B, which shows a 6-week-old balb/c mouse treated with siRNA/^{111}In-DTPA−PEI25k−PEG(2k)$_{10}$ polyplexes, radioactive signal could still be observed in the mouth and the upper trachea 24 h post treatment, and excretion via the kidneys was slightly visible. Another 24 h later (Figure 4C), radiolabeled material was obviously excreted via the kidneys, and liver deposition became slightly visible (See Supporting Information for 3D images). But the strongest signal was still observed in the lung; and only in the lower trachea radioactive material was still present. Labeled siRNA did not show accumulation in the kidneys but higher signals in the bladder and urine, as shown in Figure 5A. For more precise quantification, animals were sacrificed 48 h post treatment, and organs were dissected for scintillation counting. Figure 5A only shows organs that demonstrated significant uptake. As already discussed for the 3D SPECT images, radioactive substance was still measurable in the trachea 48 h after instillation. Interestingly, the residence time in the trachea decreased with PEGylation and was only detectable for polymers, not for siRNA. This can be explained by the interaction of the polymer with both mucus and cell surfaces, while siRNA was possibly released from the complex and was then most probably degraded and

(41) Cryan, S. A.; Sivadas, N.; Garcia-Contreras, L. In vivo animal models for drug delivery across the lung mucosal barrier. *Adv. Drug Delivery Rev.* **2007**, *59*, 1133–51.
(42) Esch, J. L.; Spektor, D. M.; Lippmann, M. Effect of lung airway branching pattern and gas composition on particle deposition. II. Experimental studies in human and canine lungs. *Exp. Lung Res.* **1988**, *14*, 321–48.
(43) Spektor, D. M.; Hunt, P. R.; Rosenthal, F.; Lippmann, M. Influence of airway and airspace sizes on particle deposition in excised donkey lungs. *Exp. Lung Res.* **1985**, *9*, 363–87.

A

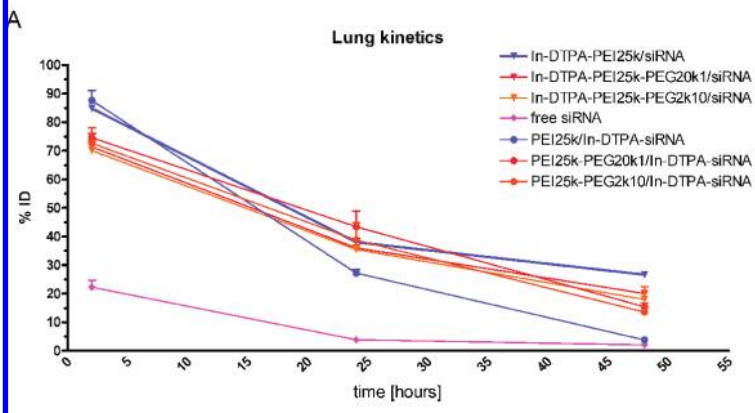

B

	free siRNA		PEI 25 kDa		PEI25k-PEG(20k)1		PEI25k-PEG(2k)10	
	scintillation	imaging	scintillation	imaging	scintillation	imaging	scintillation	imaging
polymer			25.7% ± 4.8	26.7% ± 2.4	12.9% ± 2.1	20.1% ± 0.6	11.3% ± 2.7	18.0% ± 9.9
siRNA	1.2% ± 0.2	2.1% ± 1.2	1.3% ± 1.4	3.8% ± 0.7	14.9% ± 3.6	15.4% ± 2.9	11.0% ± 3.2	13.6% ± 4.7

Figure 6. (A) Kinetic profiles of radioactively labeled compounds in the lungs over 48 h acquired by planar gamma camera imaging. (B) Comparison of data obtained by noninvasive imaging and scintillation counting of residual radioactivity in the lungs 48 h post instillation.

cleared from the trachea. As already discussed above, the deposition of instilled material depends strongly on the position of the tubus and the murine lung anatomy, and aerosolization would yield a more even distribution throughout the whole organ.[41] Due to handling of radioactive materials, we decided to use instillation, which is a commonly used technique as well.[2,23,37,44] The disadvantages of liquid instillation are clearly local irritations evoked by intubation, the stress that the liquid bolus causes, of which an unknown amount may be coughed up or swallowed, and the nonuniform distribution due to the position of the application device in the trachea during delivery affecting the percentage of material deposited in the different lung lobes.[45]

Especially in the group of mice treated with ^{111}In-DTPA−PEI25k/siRNA, a strong discrepancy between deposition to the left and right lobes was observed, which was only minor in all other groups. Interestingly, unmodified PEI 25 kDa remained in the lung to the greatest extent of all compounds labeled (total left + right lobe: 25.7% ID, compare Figure 6B), while the two PEGylated polymers showed only about half the dose left after 48 h. This again can be explained by stronger interaction of unmodified PEI with mucus and especially cell membranes which might cause sticking of the polymer. Another indication which corroborates this assumption is the fact that PEI25k-complexed siRNA did not remain in the lung to a greater extent than free siRNA. Apparently, 48 h after application, all siRNA complexed with PEI 25 kDa was released from the polymer that possibly, after penetration of mucus, interacted strongly with cells and did not behave any differently from free siRNA. PEG−PEI/siRNA complexes, on the other hand, showed lower total retention but equivalent percentages of polymer and siRNA left after 48 h. This let us hypothesize that PEG−PEI complexes were more stable after intratracheal application than PEI complexes, and this hypothesis will further be discussed below in the context of lung kinetics. Additionally to stability in vivo, another point that was crucial in our study was the circumvention of the first-pass effect, which is known to be fairly high for cationic carriers, due to rapid uptake by the reticuloendothelial system (RES).[46] Here we showed that liver uptake, which was very prominent after iv injection of the same polyplexes,[22] was strongly decreased to about 5% ID of polymers and negligible amounts of siRNA. Interestingly, kidney accumulation of polymers increased with PEGylation, which was the other way round after systemic application.[22] This surprising effect can be explained, though, by the large amount of unmodified PEI which remained in the lung and the lower systemic availability and renal excretion. Labeled siRNA, on the other hand, did not accumulate in the kidneys

(44) Lomas-Neira, J. L.; Chung, C. S.; Wesche, D. E.; Perl, M.; Ayala, A. In vivo gene silencing (with siRNA) of pulmonary expression of MIP-2 versus KC results in divergent effects on hemorrhage-induced, neutrophil-mediated septic acute lung injury. *J. Leukocyte Biol.* **2005**, *77*, 846–53.

(45) Burnell, P. K. P.; Kidger, J.; Gascoigne, M.; Kotzer, C. Powder deposition in rats assessed in vivo and in silico. In *Respiratory Drug Delivery X*; Dalby, R. N., Byron, P. R., Peart, J., Suman, J., Farr, S., Eds.; Davis Healthcare International Publishing, LCC: River Grove, IL, 2006; Vol. X, pp 625−627.

(46) Fenske, D. B.; MacLachlan, I.; Cullis, P. R. Long-circulating vectors for the systemic delivery of genes. *Curr. Opin. Mol. Ther.* **2001**, *3*, 153–8.

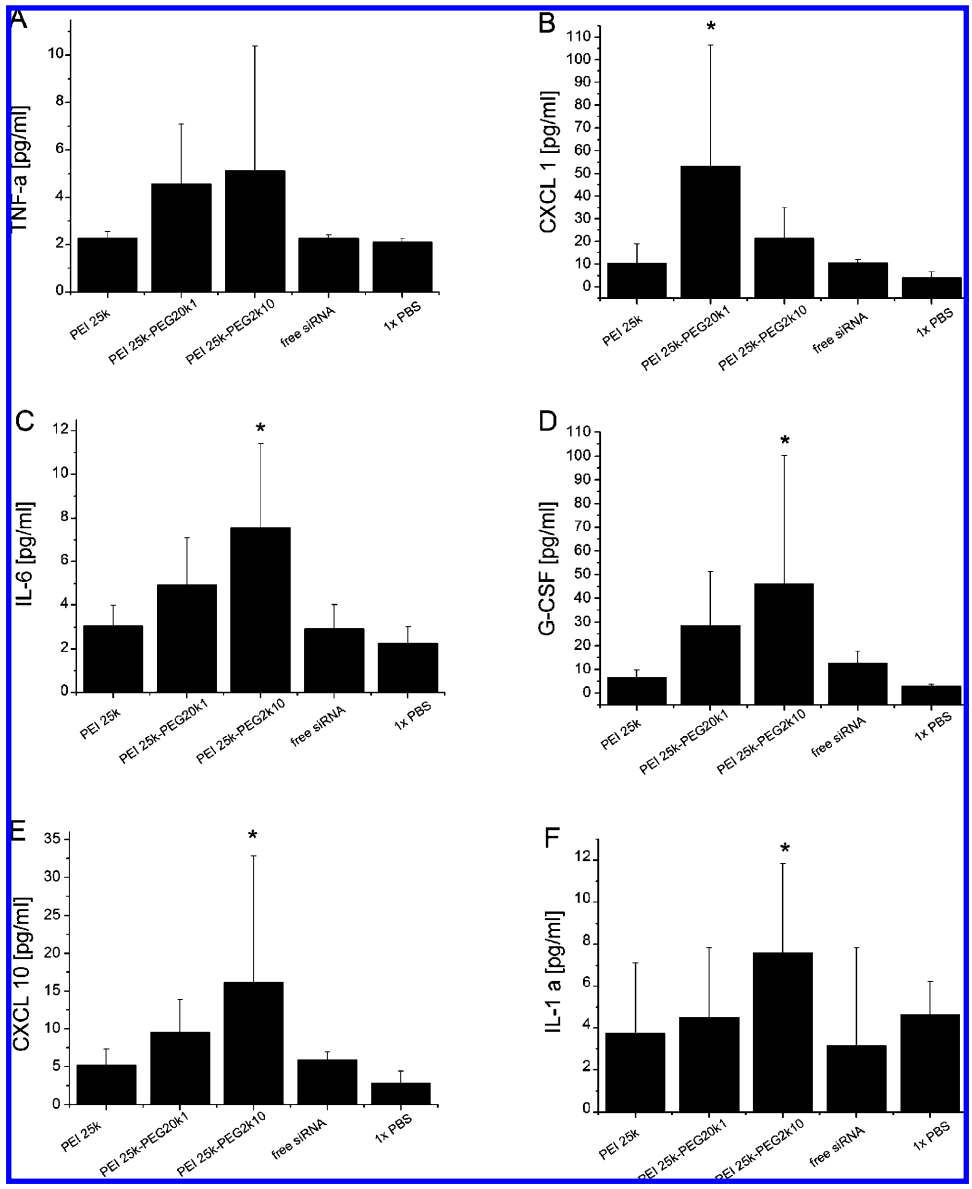

Figure 7. (A−F) Cytokine release in BALF 48 h after intratracheal instillation of siRNA polyplexes. Data represent mean ± SD ($n = 8$ for treatment with PEI polyplexes, $n = 4$ for controls (free siRNA and 1× PBS); significantly increased cytokine levels compared to control (1× PBS) were marked with an asterisk (*$p < 0.05$).

but was found in the urine. This trend is fully in line with our earlier report that showed that (PEG)−PEI/siRNA polyplexes that reach the circulation dissociate, with the polymer accumulating in liver and kidneys and the siRNA being excreted into the urine.[22] Systemic availability of all labeled compounds was measured in blood samples collected over 2 h post application. While earlier systemic availability of pulmonary applied nanoparticles was only attributed to phagocytosis by macrophages in the deep lung,[47] translocation of inhaled particles is now being studied by several groups who have demonstrated transcytosis[48] or transport of systemically available particles into the brain via olfactory nerves after pulmonary application.[49] One concern we thoroughly addressed, in order to avoid misleading pharmacokinetic data, is purification of the labeled material. With our optimized 2-step purification procedure,[21] we are able to ensure that no free radiometal ions are present in the complex solution. Free indium or DTPA−indium would not accumulate in the liver or kidneys either, so we are rather sure that the systemically available radioactivity was not free

(47) Nemmar, A.; Vanbilloen, H.; Hoylaerts, M. F.; Hoet, P. H.; Verbruggen, A.; Nemery, B. Passage of intratracheally instilled ultrafine particles from the lung into the systemic circulation in hamster. *Am. J. Respir. Crit. Care Med.* **2001**, *164*, 1665–8.

(48) Kato, T.; Yashiro, T.; Murata, Y.; Herbert, D. C.; Oshikawa, K.; Bando, M.; Ohno, S.; Sugiyama, Y. Evidence that exogenous substances can be phagocytized by alveolar epithelial cells and transported into blood capillaries. *Cell Tissue Res.* **2003**, *311*, 47–51.

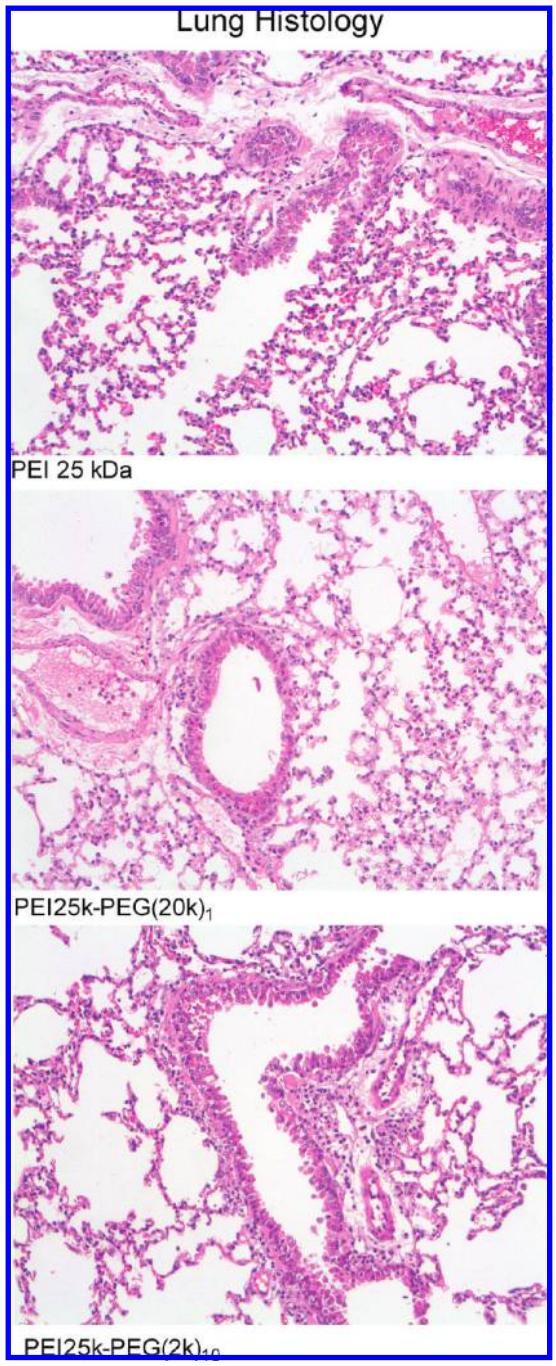

Figure 8. Light microscopy dislosed normal lung tissue. The bronchiolar and alveolar epithelium appeared normal, and the interstitium and alveolar lumina showed no inflammation.

label. Systemically available free siRNA is known to be excreted faster than degraded,[1] although it is possible that part of the signal in the urine was caused by degradation of nucleic acids. Full length siRNA can be re-extracted from tissue, blood or urine samples and quantified, e.g. by autoradiography,[50] which will be subject to a more thorough investigation which is currently underway. Although uptake of labeled siRNA into the circulation seemed to be very similar, no matter which polymer was used for complexation (Figure 5B), calculation of the area under the curve (AUC) (Figure 5D) revealed the following differences: While PEI 25 kDa complexed siRNA was available to the lowest extent in the first 20 min, which corroborates our data from the stability assay, the release of siRNA seemed to be delayed, and systemic availability surpassed that of free siRNA 1 h after administration. PEG−PEI complexed siRNA, on the other hand, exhibited higher initial blood concentrations, according to their stability profiles shown in Figure 3, which did not further increase but even decreased in the case of PEI25k−PEG$(2k)_{10}$ complexed siRNA. The decrease in systemic availability can easily be explained by extensive excretion into the urine, as shown in Figure 5A. Polymers that were endocytosed or transcytosed from the lung were deposited in the liver and kidneys to a greater extent than their payload, as demonstrated in Figure 5A. This also revealed shorter circulation and lower AUC values. PEI 25 kDa, which was strongly retained in the lung, was only to a low extent taken up into circulation. The decrease in blood levels after 1 h post application can be attributed to liver and kidney accumulation. PEI25k−PEG$(20k)_1$ showed increasing systemic availability over 20 min post instillation followed by a steady state concentration. This polymer, equipped with one long PEG chain, is possibly least prone to recognition by liver macrophages or interaction with the cationic basal membrane in the kidneys. The systemic concentration of PEI25k−PEG$(2k)_{10}$ increased more slowly but was also followed by a steady state concentration after 1 h post application. The lower AUC and the slower increase of blood levels can be explained by stronger liver and kidney accumulation shown in Figure 5A and Figures 4B and 4C. Overall, AUC values of polymers were significantly lower than those of siRNA ($^{**}p < 0.01$, Figure 5D). No differences were observed among the different polymers, but differences were more striking concerning siRNA. Due to the strong increase in blood levels of PEI 25 kDa complexed siRNA after 20 min post application, AUC of free and PEI 25 kDa complexed siRNA were not significantly different. The AUC of PEI25k−PEG$(20k)_1$ complexed siRNA was not significantly lower, whereas the decreased AUC of the PEI25k−PEG$(2k)_{10}$ complexed siRNA was significant ($^{*}p < 0.05$, Figure 5D), which was certainly an effect of excretion and stronger initial stability of the complexes, as also demonstrated in Figure 1B.

While end point scintillation counting of dissected lungs only revealed residual concentration after sacrifice of the animals (Figure 5A), SPECT and planar gamma camera imaging enabled noninvasive imaging and quantification of the retention of radiolabeled material in the same animal over time. Scintillation counting analysis suggested that complexation of siRNA with PEI 25 kDa did not provide any benefit over application of free siRNA. If considering the kinetics of residual radioactivity in the lung over time, the

(49) Oberdorster, G.; Sharp, Z.; Atudorei, V.; Elder, A.; Gelein, R.; Lunts, A.; Kreyling, W.; Cox, C. Extrapulmonary translocation of ultrafine carbon particles following whole-body inhalation exposure of rats. *J. Toxicol. Environ. Health A* **2002**, *65*, 1531–43.

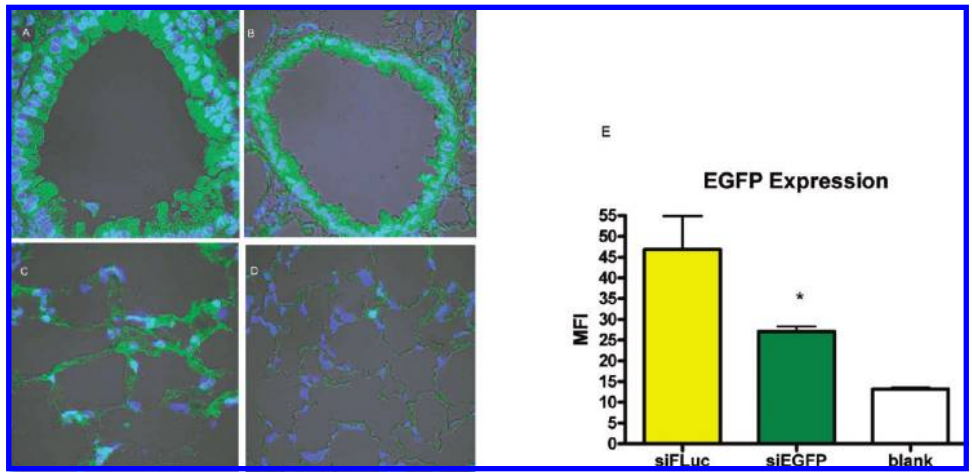

Figure 9. Knockdown in actin-EGFP mice. (A) Bronchiolus of a control EGFP-mouse displaying high fluorescence intensity. (B) Bronchiolus of a PEI25k−PEG(2k)$_{10}$/siRNA treated EGFP-mouse displaying lower fluorescence intensity. (C) Alveolar epithelium of a control EGFP-mouse displaying high fluorescence intensity. (D) Alveolar epithelium of a PEI25k−PEG(2k)$_{10}$/siRNA treated EGFP-mouse displaying almost complete loss of fluorescence signal. (E) Knockdown in actin-EGFP mice compared to non-EGFP-expressing mice (blank). EGFP-expression in lungs of siEGFP/PEI(25k)−PEG(2k)$_{10}$ treated mice was downregulated by 42% and is significantly ($p < 0.05$) lower than in mice treated with siFLuc/PEI(25k)−PEG(2k)$_{10}$.

picture looks a bit different: Although in the stability assay PEI complexes seemed to be most stable, it certainly has to be acknowledged that stability over time, and especially in high ionic strength solutions, might be lower than in the in vitro assay. We already discussed increasing blood levels of PEI 25 kDa complexed siRNA after 20 min post instillation, letting us assume that the polyplexes were stable in the presence of mucus and surfactant, but the release of siRNA obviously occurred to a later time point: possibly when polyplexes reached the cells and strongly interacted with cell surfaces. The analysis of radioactivity signals in the lungs taken by planar gamma camera imaging and analysis of ROIs very well corroborated this assumption (Figure 6A). Whereas the amount of radioactively labeled PEI 25 kDa decreased slowly over 48 h, that of PEI 25 kDa complexed siRNA decreased more rapidly than PEG−PEI complexed siRNA. The curves for PEG−PEI polymer and the corresponding payload showed very similar behavior. The analysis of three time points certainly cannot be considered a pharmacokinetic study, but as shown in Figure 6B, data acquired in the imaging approach coincides well enough with that obtained from dissected organs to make a noninvasive prediction of the retention of labeled material in the lung. Most importantly, we were able to prove our assumption that PEG−PEI/siRNA complexes are more suitable for lung application than PEI/siRNA complexes concerning protection of siRNA and residing times in the lung.

Bronchoalveolar Lavage. Since there are various reports in the literature stating that cationic lipids used for pulmonary gene delivery result in immune and cytokine responses in mice,[51,52] whereas aerosol delivery of PEI/DNA complexes did not induce high levels of cytokines,[53] we investigated the effect of our siRNA loaded nanocarriers. Interestingly, as shown in Figure 7, our PEI/siRNA complexes had the lowest proinflammatory effect, whereas PEI25k−PEG(20k)$_1$ complexes caused a 13-fold increase of CXCL1 (53.2 pg/mL ± 53.3 vs 4.1 pg/mL ± 2.6), 2-fold elevated levels of IL-6 (4.9 pg/mL 2.2 vs 2.3 pg/mL ± 0.8) and a 2.5-fold increase of TNF-α (4.5 pg/mL ± 2.5 vs 2.1 pg/mL ± 0.2) in the BALF. PEI(25)−PEG(2k)$_{10}$ complexes caused a 1.5-fold increase of CXCL1 (21.4 pg/mL ± 13.8 vs 4.1 pg/mL ± 2.6), a 3-fold increase of IL-6 (7.5 pg/mL ± 3.8 vs 2.3 pg/mL ± 0.8) and a 2.5-fold increase of TNF-α levels (5.2 pg/mL ± 5.5 vs 2.1 pg/mL ± 0.2). In addition to the acute phase cytokine response, the release of granulocyte-colony stimulating factor (G-CSF) and the interferon-γ inducible protein 10 (CXCL10) was more than ten times elevated for PEI(25)−PEG(2)$_{10}$ compared to control (1× PBS treated mice), G-CSF (46.3 pg/mL ± 54.0 vs 3.1 pg/mL ± 0.7) and CXCL10 (16.2 pg/mL ± 16.7 vs 2.8 pg/mL ± 1.6). The PEGylated nanocarriers were therefore considered to have a moderate proinflammatory effect which was more prominent for PEI(25)−PEG(2)$_{10}$. Concerning differential analysis of BAL cells, the two PEG-modified PEI nanocarriers caused more than 20% recruitment of polymorphonuclear neutrophilic granulocytes (PMN), which is regarded as a hallmark of lung inflammation especially for the 48 h response (data not shown). BAL cells of mice treated with PEI 25 kDa/siRNA polyplexes, on the other hand, were exclusively macrophages, in accordance with the cytokine profile where we could not detect elevated levels of acute phase cytokines. It has to be remarked, though, that BAL was performed 48 h post instillation, but cytokine levels in the BALF were reported to peak at 24 h after PEI/DNA aerosol exposure.[53] A kinetic analysis as performed in the latter report will be part of our kinetic study concerning gene silencing.

(50) Malek, A.; Merkel, O.; Fink, L.; Czubayko, F.; Kissel, T.; Aigner, A. In vivo pharmacokinetics, tissue distribution and underlying mechanisms of various PEI(-PEG)/siRNA complexes. *Toxicol. Appl. Pharmacol.* **2009**, *236*, 97–108.

Lung Histology. While nanomedicine is an emerging and promising field, possible health risks need to be considered as well. Application of nanomaterials to the lung often evokes an allusion to the effects of asbestos fibers on lung tissue. Indeed, also carbon black nanoparticles have been shown to bear health risks by interfering with cell signaling.[54] The airways are a relatively robust barrier, being protected by a viscous layer of mucus and equipped with an effective clearance mechanism, but alveoli are presumably more prone to damage. In the alveolar region, macrophage phagocytosis is the main mechanism of clearance, but nanosized particles are designed not to be recognized by alveolar macrophages, which possibly might increase their irritating or toxic effects. In the case of positively charged particles, interaction with and toxic effects on cell membranes are well-known and studied.[55] Concerning lung toxicity, it has been shown that the three-dimensional structure and flexibility of the macromolecules has a strong impact on accessibility of charges and thus on their cytotoxic profiles.[56] In order to study the impact of our nanocarriers, which have already been characterized for in vitro toxicity (Beyerle et al., in preparation), on lung tissue in vivo, we fixed dissected lungs in paraformaldehyde and analyzed paraffin sections after H&E staining. As demonstrated in Figure 8, we did not observe indications of inflammation in any of the lungs investigated at the light microscopic level. It has to be acknowledged, though, that chronic effects cannot be precluded based on a single application and observation for just 48 h.

In Vivo Knockdown. In order to confirm that intratracheal siRNA delivery leads to effective intracellular siRNA concentration and functional activity, we treated actin-EGFP expressing mice with polyplexes containing 50 μg of anti-EGFP siRNA. This dose has been reported to be efficient in downregulation of EGFP in the same mouse strain after high pressure tail vein (HPTV) injection,[57] and is below the dose that has been reported to be effective after intratracheal instillation.[44] Due to the sustained retention of the polyplexes in the lung, mice were sacrificed 5 days after instillation, and lungs were paraffin embedded after fixation in paraformaldehyde. In a preliminary study (data not shown) we compared fluorescence of paraffin sections to cryo sections in order to check on any adverse effects of paraformaldehyde or paraffin on fluorescence intensity. Neither revealed disadvantages, but cells in paraffin sections retained their morphology much better than those in cryo sections, which encouraged us to embed all lungs for this study in paraffin. CLSM allowed us to qualitatively investigate the effects of anti-EGFP siRNA on the expression of EGFP. Figure 9A shows a bronchiolus of an untreated actin-EGFP mouse, where especially type II pneumocytes, but also all surrounding cells, exhibit high fluorescence intensity. In the siRNA-treated mouse, fluorescence intensity in the bronchial cells seemed to be decreased (Figure 9B), and the effect becomes more apparent in the alveolar cells of nontreated (Figure 9C) versus treated animals (Figure 9D). Although we are well aware that this microscopic indication needs to be quantified in order to test the hypothesis, at this point we can safely assume that polyplexes reached the alveoli after instillation and are taken up into alveolar tissue where they are released into the cytosol in sufficient concentration for functional activity. In a first approach to quantify the knockdown of EGFP expression, we have treated EGFP-expressing mice with PEG−PEI complexed specific (siEGFP) and nonspecific (siFLuc) siRNA and measured EGFP in total lung homogenates. EGFP expression was found to be 42% knocked down compared to siFLuc-treated animals and thereby significantly ($*p < 0.05$) reduced, and not significantly different from animals that do not express EGFP at all but only show autofluorescence of macrophages ($p > 0.05$). A thorough follow-up study investigating the time-course and dose-dependency of polyplexes made of the different polymers and the fractionation of lung homogenates into different populations of cells will provide more details.

Conclusions

In conclusion, we have shown that 25/27mer partial 2′-OMe modified DsiRNA can be efficiently condensed with PEI and PEG−PEI. From our direct condensation assay we have learned that this type of experiment reveals data that has to be critically interpreted. We have disclosed that PEI/siRNA polyplexes are more stable than PEG−PEI/siRNA polyplexes over 20 min in the presence of mucin or surfactant under in vitro conditions. By comparison of planar imaging with conventional scintillation counting techniques, we showed that, for the understanding of the behavior of nanocarriers in vivo, simple end point measurements are

(51) Li, S.; Wu, S. P.; Whitmore, M.; Loeffert, E. J.; Wang, L.; Watkins, S. C.; Pitt, B. R.; Huang, L. Effect of immune response on gene transfer to the lung via systemic administration of cationic lipidic vectors. *Am. J. Physiol.* **1999**, *276*, L796–804.

(52) Freimark, B. D.; Blezinger, H. P.; Florack, V. J.; Nordstrom, J. L.; Long, S. D.; Deshpande, D. S.; Nochumson, S.; Petrak, K. L. Cationic lipids enhance cytokine and cell influx levels in the lung following administration of plasmid: cationic lipid complexes. *J. Immunol.* **1998**, *160*, 4580–6.

(53) Gautam, A.; Densmore, C. L.; Waldrep, J. C. Pulmonary cytokine responses associated with PEI-DNA aerosol gene therapy. *Gene Ther.* **2001**, *8*, 254–7.

(54) Brown, D. M.; Donaldson, K.; Borm, P. J.; Schins, R. P.; Dehnhardt, M.; Gilmour, P.; Jimenez, L. A.; Stone, V. Calcium and ROS-mediated activation of transcription factors and TNF-alpha cytokine gene expression in macrophages exposed to ultrafine particles. *Am. J. Physiol.* **2004**, *286*, L344–53.

(55) Hong, S.; Leroueil, P. R.; Janus, E. K.; Peters, J. L.; Kober, M. M.; Islam, M. T.; Orr, B. G.; Baker, J. R., Jr.; Banaszak Holl, M. M. Interaction of polycationic polymers with supported lipid bilayers and cells: nanoscale hole formation and enhanced membrane permeability. *Bioconjugate Chem.* **2006**, *17*, 728–34.

(56) Singh, A. K.; Kasinath, B. S.; Lewis, E. J. Interaction of polycations with cell-surface negative charges of epithelial cells. *Biochim. Biophys. Acta* **1992**, *1120*, 337–42.

(57) Wesche-Soldato, D. E.; Chung, C. S.; Lomas-Neira, J.; Doughty, L. A.; Gregory, S. H.; Ayala, A. In vivo delivery of caspase-8 or Fas siRNA improves the survival of septic mice. *Blood* **2005**, *106*, 2295–301.

insufficient. While data obtained by both methods coincided well, 3D and planar imaging enabled tracking the biodistribution over time. Although PEI/siRNA complexes seemed to be most stable in the in vitro stability assays, their in vivo performance was poor with PEI being left in the lungs and the siRNA payload released and excreted. Despite their slightly higher proinflammatory potential, we favored PEG−PEI/siRNA complexes for investigation of functional gene silencing activity in vivo for sustained release reasons and were able to report indications of success with no histological abnormality detected. These results are very encouraging for further investigation and quantification of in vivo gene silencing in the lung after intratracheal instillation of PEG−PEI/siRNA complexes.

Acknowledgment. We are grateful to Prof. Renz and Dr. Garn (Department of Clinical Chemistry, Philipps-Universität Marburg) for the generous use of equipment and facilities, to Viktoria Morokina (Department of Pathology, University Hospital Giessen-Marburg) and Klaus Keim (Department of Pharmaceutics and Biopharmacy, Philipps Universität Marburg) for excellent technical support and to Thomas Carlsson (Department of Experimental Neurology, Philipps Universität Marburg) for supplying us with actin-GFP expressing mice. Deutsche Forschungsgemeinschaft (DFG Forschergruppe 627), MEDITRANS, an Integrated Project funded by the European Commission under the Sixth Framework (NMP4-CT-2006-026668), and the German Lung Foundation (Deutsche Lungenstiftung e.V.) are gratefully acknowledged.

Supporting Information Available: 3D images (.avi format) as described in the text. This material is available free of charge via the Internet at http://pubs.acs.org.

MP900107V